

The Utility of a Novel Proximal Femur Maturity Index for Staging Skeletal Growth in Patients with Idiopathic Scoliosis

Prudence Wing Hang Cheung, BDS(Hons), Federico Canavese, MD, PhD, Chris Yin Wei Chan, MD, MSOrth, Janus Siu Him Wong, MBBS, MRCSEd, Hideki Shigematsu, MD, PhD, Keith Dip Kei Luk, MBBS, MCh(Orth), FRCSEd, FRACS, FHKCOS, FHKAM, and Jason Pui Yin Cheung, MBBS, MMedSc, MS, PDipMDPath, MD, MEd, FRCSEd, FHKAM, FHKCOS

Investigation performed at the Department of Orthopaedics and Traumatology, The University of Hong Kong, Pokfulam, Hong Kong SAR

Background: For growing patients, it is ideal to have a growth plate visible in routine radiographs for skeletal maturity assessment without additional radiation. The proximal femoral epiphyseal ossification is in proximity to the spine; however, whether it can be used for assessing a patient's growth status remains unknown.

Methods: Two hundred and twenty sets of radiographs of the spine and the left hand and wrist of patients with idiopathic scoliosis were assessed for skeletal maturity and reliability testing. Risser staging, Sanders staging (SS), distal radius and ulna (DRU) classification, the proximal humeral ossification system (PHOS), and the novel proximal femur maturity index (PFMI) were used. The PFMI was newly developed on the basis of the radiographic appearances of the femoral head, greater trochanter, and triradiate cartilage. It consists of 7 grades (0 to 6) associated with increasing skeletal maturity. The PFMI was evaluated through its relationship with pubertal growth (i.e., the rate of changes of standing and sitting body height [BH] and arm span [AS]) and with established skeletal maturity indices. Longitudinal growth data and 780 corresponding spine radiographs were assessed to detect peak growth using receiver operating characteristic (ROC) curve analysis.

Results: The PFMI was found to be correlated with chronological age ($\tau_b = 0.522$), growth rates based on standing BH ($\tau_b = -0.303$), and AS ($\tau_b = -0.266$) ($p < 0.001$ for all). The largest growth rate occurred at PFMI grade 3, with mean standing BH growth rates (and standard deviations) of 0.79 ± 0.44 cm/month for girls and 1.06 ± 0.67 cm/mo for boys. Growth rates of 0.12 ± 0.23 cm/mo (girls) and 0 ± 0 cm/mo (boys) occurred at PFMI grade 6, indicating growth cessation. Strong correlations were found between PFMI gradings and Risser staging ($\tau_b = 0.743$ and 0.774 for girls and boys), Sanders staging ($\tau_b = 0.722$ and 0.736 , respectively), and radius ($\tau_b = 0.792$ and 0.820) and ulnar gradings ($\tau_b = 0.777$ and 0.821), and moderate correlations were found with PHOS stages ($\tau_b = 0.613$ and 0.675) ($p < 0.001$ for all). PFMI gradings corresponded to as young as SS1, R4, U1, and PHOS stage 1. Fair to excellent interrater and intrarater reliabilities were observed. PFMI grade 3 was most prevalent and predictive for peak growth based on ROC results.

Conclusions: The PFMI demonstrated clear pubertal growth phases with satisfactory reliability. Grade 3 indicates peak growth and grade 6 indicates growth cessation.

Clinical Relevance: The use of PFMI can benefit patients by avoiding additional radiation in skeletal maturity assessment and can impact current clinical protocol of patient visits. PFMI gradings had strong correlations with SS, DRU gradings, and Risser staging, and they cross-referenced to their established grades at peak growth and growth cessation. PFMI may aid in clinical decision making.

Disclosure: The **Disclosure of Potential Conflicts of Interest** forms are provided with the online version of the article (<http://links.lww.com/JBJS/G875>).

Copyright © 2022 The Authors. Published by the Journal of Bone and Joint Surgery, Incorporated. All rights reserved. This is an open-access article distributed under the terms of the [Creative Commons Attribution-Non Commercial-No Derivatives License 4.0](https://creativecommons.org/licenses/by-nc-nd/4.0/) (CCBY-NC-ND), where it is permissible to download and share the work provided it is properly cited. The work cannot be changed in any way or used commercially without permission from the journal.

Paediatric spinal and limb deformities require accurate assessment of remaining growth potential. Determining when peak height velocity (PHV) and the period of growth cessation occur is crucial for prompt brace intervention and weaning for scoliosis management^{1,2} and for epiphysiodesis or limb-lengthening surgery³⁻⁵. As chronological age is not accurate in indicating the timing of pubertal growth landmarks such as PHV⁶, skeletal bone age is an essential measure along with secondary sexual characteristics⁷. Skeletal maturity status can be a crucial factor for treatment prognosis and an indicator for the risk of curve progression⁷⁻¹⁰.

There are multiple skeletal maturity measures currently in use for assessing growth, including Risser staging¹¹, triradiate cartilage closure¹²⁻¹⁴, Sanders staging (SS)¹⁵, the distal radius and ulna (DRU) classification¹⁶, and the proximal humeral ossification system (PHOS)¹⁷. Unlike the poor sensitivity of Risser staging for predicting PHV^{18,19}, SS and the DRU classification have been found to be effective for indicating peak growth^{7,14,20}, predicting curve progression in adolescent idiopathic scoliosis (AIS)^{21,22}, and deciding when to wean from brace wear²³. Despite these advantages, assessment requires a hand and wrist radiograph, resulting in additional radiation exposure. The use of the proximal humeral ossification center was previously explored; however, there are difficulties in its visualization without distortion because of the current standards of arm positioning for radiographs with fists on clavicles but arms slightly forward for better visibility of the sagittal spinal alignment²⁴. Conversely, physes at the pelvis can be considered for skeletal maturation assessment as the parameters of the pelvis and the spine were found to be correlated in previous studies^{25,26}.

With the advent of biplanar stereoradiography, whole body images with complete visibility of the proximal femoral epiphysis are feasible without gonadal shields²⁷. This growth plate has the benefits of viewing convenience on spine radiographs and its proximity to the axial skeleton. Thus, additional radiation exposure is minimized. Currently, an established grading system for bone age based on spine radiographs is lacking for patients with spinal deformities. For the patients with slipped capital femoral epiphysis²⁸, the modified Oxford bone score incorporating 5 radiographic features of the pelvis (i.e., the ilium, triradiate cartilage, femoral head, and the greater and lesser trochanters) is used for predicting the risk of contralateral slip²⁹. The score is complex as each anatomical feature has 3 maturation stages, and it may not be suitable for quick assessment.

The present study aimed to develop a proximal femur maturity index (PFMI), which incorporated the appearance of the femoral head, greater trochanter, and triradiate cartilage for growth assessment. The PFMI was investigated by (1) evaluating the relationship of the PFMI gradings with pubertal growth, (2) assessing the relationship of PFMI with other maturity parameters, and (3) determining how the index covers the pubertal growth period.

Materials and Methods

Study Design

Patients who were referred to our tertiary scoliosis clinic with the diagnosis of idiopathic scoliosis from February

2016 to February 2019 were considered for recruitment. All skeletally immature patients with Risser stage 0 at first consultation were included. Patients were required to have a left hand-and-wrist radiograph and a posteroanterior spine radiograph made on the same day as the initial consultation and on any subsequent visit (see Appendix 1). Exclusion criteria included patients with growth hormone deficiency or developmental delay, or those at a Risser stage of ≥ 1 at initial assessment (Fig. 1). Ethics committee approval and informed consent of the parent(s) or guardians of the enrolled patients were obtained.

Data collection included patients' chronological age, sex, date of menarche for girls, standing and sitting body height (BH), arm span (AS), and body weight. The coronal Cobb angles were measured by the attending orthopaedic specialist during each visit. Skeletal maturity was assessed every 4 to 6 months throughout the treatment period using Risser staging³⁰ (from stage 0 to 5, with stage 0– indicating open triradiate cartilage and stage 0+ indicating closed triradiate cartilage³¹), SS (ranging from SS1 to SS8)⁷, DRU classification (radius grades from R1 to R11 and ulnar grades from U1 to U9)¹⁶, and PHOS (stage 1 to 5)¹⁷.

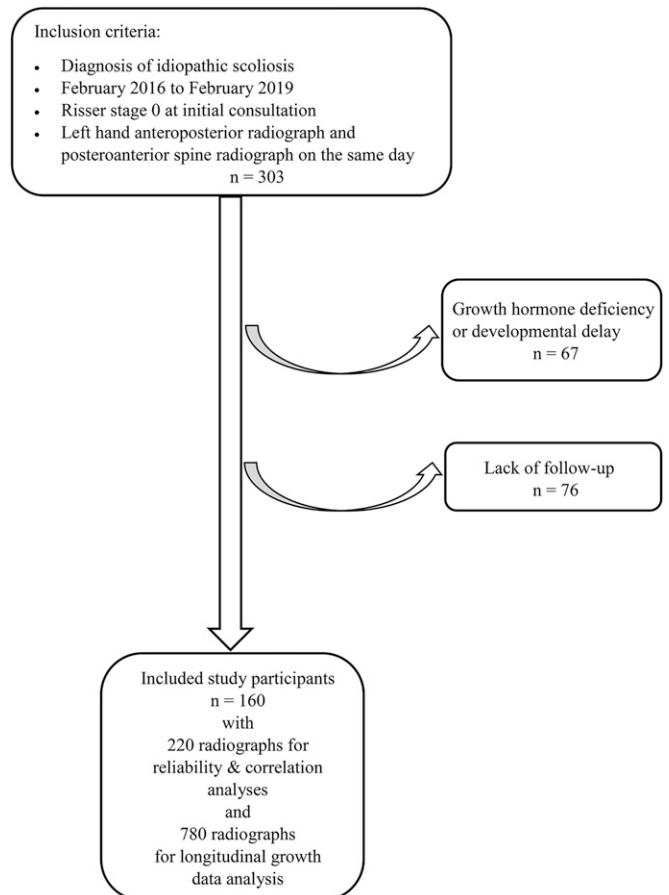


Fig. 1
Flowchart of patient recruitment.

Proximal Femur Maturity Index





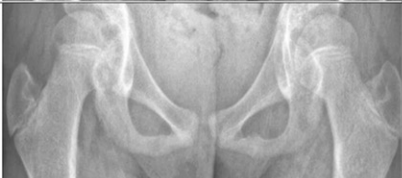









Grade	Stage	Femoral head	Greater trochanter	Triradiate cartilage	Example of radiographs	Schematic diagrams
0	Pre-adolescent	Epiphysis smaller than metaphysis	Smooth in shape	Open		
1	Acceleration phase	Epiphysis larger than metaphysis	Tapered in shape	Open		
2	Pre-peak	Lateral physeal beaking	Triangular-shaped	Open		
3	Peak growth spurt	<ul style="list-style-type: none"> • Medial physeal beaking with lateral side already beaking or closed • Oblique/ curved physis 	Trochanteric notch visible or Double contour line over piriformis fossa	Open/Closed		
4	Post-peak	Narrowing of the physeal plate or partial fusion	Fusion of middle of physis	Closed		
5	Growth deceleration	Closed physis with visible scar	Complete closure	Closed		
6	Maturity	Complete closure	Complete closure	Closed		

Fig. 2
Proximal femur maturity index.

Defining the Stages for the Proximal Femur Maturity Index

For the recruited patients, 1 experienced orthopaedic surgeon (J.P.Y.C.) examined the radiographic appearances of the femoral head, greater trochanter, and respective triradiate cartilage in the spine radiographs. Any recurring pattern of radiographic presentation of the physes was summarized in words as descriptors of different stages from open toward physeal clo-

sure. This formed the preliminary framework of grading for the new maturity index. Six orthopaedic surgeons converged as the expert panel to develop the descriptions into specific wordings that were refined as appropriate maturation grades via consensus.

The PFMI consists of grades 0 to 6 (Fig. 2, Table I). Each grade is composed of an assessment of the femoral head

TABLE I Radiographic Characteristics of the PFMI Grades*

Grade	Radiographic Characteristics†
0	The femoral head epiphysis is smaller than the metaphysis (a tangential line along the femoral neck does not overlap with the epiphysis).
1	The epiphysis is wider than the metaphysis at the femoral head.
2	Lateral physeal beaking of the femoral epiphysis, with a triangular greater trochanter, is evident.
3	Medial physeal beaking occurs at the femoral head, with the lateral side beaking or closed. The greater trochanteric notch or the double contour line over the piriformis fossa is now visible.
4	The physeal plate of the femoral head begins to narrow or fuse partially, with closure of the triradiate cartilage. The middle of the physis at the greater trochanter is also fused.
5	Both medial and lateral sides of the femoral head physeal plate and of the greater trochanter are closed. Only a scar is still visible at the femoral head.
6	Physes of both the femoral head and greater trochanter are completely fused.

*PFMI = proximal femur maturity index. †In the case of any discrepancy between the right and left sides, the earlier, less mature grade is used.

and the greater trochanter and incorporates both of those anatomical features and the triradiate cartilage for the final grading.

Reliability Test

Two hundred and twenty spine radiographs from the recruited patients were prepared by an investigator (P.W.H.C.) who was not involved in the grading process. Multiple radiographs could be extracted from one patient. The same panel of 6 orthopaedic surgeons assessed the grades independently. They were blinded to patients' demographic and growth data and the hand-and-wrist bone age, which was graded during the consultation. The radiographs were then randomized and presented after 2 weeks for another assessment.

Outcome Measures

Bodily growth rate was assessed by the change of the standing BH, sitting BH, or AS between the day of maturity assessment and the following visit, divided by the time interval elapsed. Most follow-up visits were scheduled at intervals of 4 to 6 months. The amount of growth that occurred following the date of skeletal maturity assessment was calculated for each radiograph from which the gradings were made, as it is important to assess the skeletal maturity measure for its predictive ability for future growth. All clinical data were retrieved from the database independently from the radiographic assessments performed by the raters.

Statistical Analysis

Data normality was tested using Shapiro-Wilk tests. Interrater and intrarater reliability were investigated using the weighted kappa coefficient, a conservative measure that takes into account the closeness of agreement³² and assesses the level of disagreement when the ratings are in ordered gradings³³, but the intervals between consecutive stagings are not necessarily equal^{34,35}. A weighted kappa coefficient (κ_w) of ≥ 0.75 indicates excellent agreement; κ_w between 0.40 and 0.75 represents fair to good agreement beyond chance, and κ_w of ≤ 0.40 represents poor agreement³⁶.

We first examined whether skeletal maturity gradings had any relationships with growth rates in the present study cohort using ranked statistics Kendall τ_b . Scatterplots were created to represent the growth rate per maturity grading to examine the grade(s) at which peak growth and growth cessation occurred. For the PFMI, we specifically compared the growth rates between PFMI gradings using Kruskal-Wallis one-way analysis of variance (ANOVA), followed by post hoc pairwise comparisons with the Bonferroni correction. Moreover, the relationship between the PFMI and each other skeletal maturity index was investigated using the Kendall τ_b correlation test³⁷. Distributions of PFMI gradings and their corresponding hand-wrist maturity gradings were explored via cross-tabulation. This allowed the examination of the range of skeletal maturity being covered by the PFMI.

Longitudinal growth data were analyzed for patients who had reached a skeletal maturity of PFMI grade 6 within the study period and demonstrated a peak in the series of growth rates. This amounted to 780 spine radiographs (608 for girls and 172 for boys) for skeletal maturity assessment using the PFMI, with an average of 7.5 visits per patient. For each patient, PFMI grading was assessed at each visit, and the timing of the greatest growth rate within that individual was indicated as peak growth. Through receiver operating characteristic (ROC) curve analysis and the area under the ROC curve, the accuracy of the model predictions of the timing of peak growth by the PFMI grading was evaluated. The cutoff PFMI grade with the highest percentage of sensitivity and specificity was determined as the most optimal grade for indicating peak growth.

A p value of < 0.05 was considered significant. Descriptive statistics and 95% confidence intervals (CIs) were reported when applicable. Statistical analyses were conducted using SPSS (version 26.0; IBM).

Source of Funding

Funding was received from the RGC Research Impact Fund (R5017-18F).

Results

A total of 160 patients (70.6% were girls) with a mean major coronal Cobb angle (and standard deviation) of $24.5^\circ \pm 10.1$ were recruited (Table II). Reliability testing of the PFMI indicated fair to good agreement between raters ($\kappa_w = 0.67$ [95% CI: 0.62 to 0.71; $p < 0.001$] for the first reader and 0.69 [95% CI: 0.65 to 0.72; $p < 0.001$]) for the second reader, with excellent intrarater reliability ($\kappa_w = 0.80$ [95% CI: 0.78 to 0.82;

TABLE II Patient Profile

	Whole Cohort	Girls	Boys
No. (%) of patients	160 (100)	113 (70.6)	47 (29.4)
No. (%) of radiographs	220 (100)	157 (71.4)	63 (28.6)
Chronological age* (yr)	12.0 ± 1.4	11.7 ± 1.3	12.6 ± 1.5
Postmenarche† (no. [%]) (n = 157)		43 (27.4)	
Months after menarche*		11.4 ± 9.1	
Standing body height* (cm)	148.8 ± 11.1	147.0 ± 10.2	153.5 ± 11.7
Arm span* (cm)	148.7 ± 11.4	146.6 ± 11.0	153.9 ± 11.0
Sitting height* (cm)	79.7 ± 5.6	78.8 ± 5.4	82.0 ± 5.6
Weight* (kg)	37.9 ± 9.1	37.2 ± 9.4	39.8 ± 8.3
Coronal Cobb angle* (major curve) (deg)			
No bracing	24.1 ± 9.7	25.3 ± 10.0	21.5 ± 8.5
Out of brace measurement at time of radiograph	31.0 ± 9.6	30.4 ± 9.6	33.8 ± 10.0
In brace measurement at time of radiograph	18.2 ± 8.8	17.5 ± 8.3	22.0 ± 11.5

*The values are given as the mean and the standard deviation. †The values are based on the number of radiographs.

$p < 0.001$]). At the 12-week reassessment of rater reliability after the introduction of the flowchart (Fig. 3) to facilitate the use of the new PFMI, an improvement of interrater reliability was achieved ($\kappa_w = 0.84$ [95% CI: 0.83 to 0.85; $p < 0.001$]), while intrarater reliability was maintained.

Significant correlations ($p < 0.001$ for all) were found between the PFMI and chronological age ($\tau_b = 0.522$) as well as

growth rates based on standing BH ($\tau_b = -0.303$) and AS ($\tau_b = -0.266$), but not with sitting BH ($\tau_b = -0.070$; $p = 0.161$), although a similar trend was observed (Fig. 4). Scatterplots revealed that the largest growth rate (in standing BH, sitting BH, and AS) occurred at PFMI grade 3 for both sexes, except for AS for boys, in which growth rates were similar for grade 2 (mean, 0.97 ± 0.71 cm/mo) and grade 3 (mean, 0.93 ± 0.50 cm/mo)

Flow chart for using the Proximal Femur Maturity Index

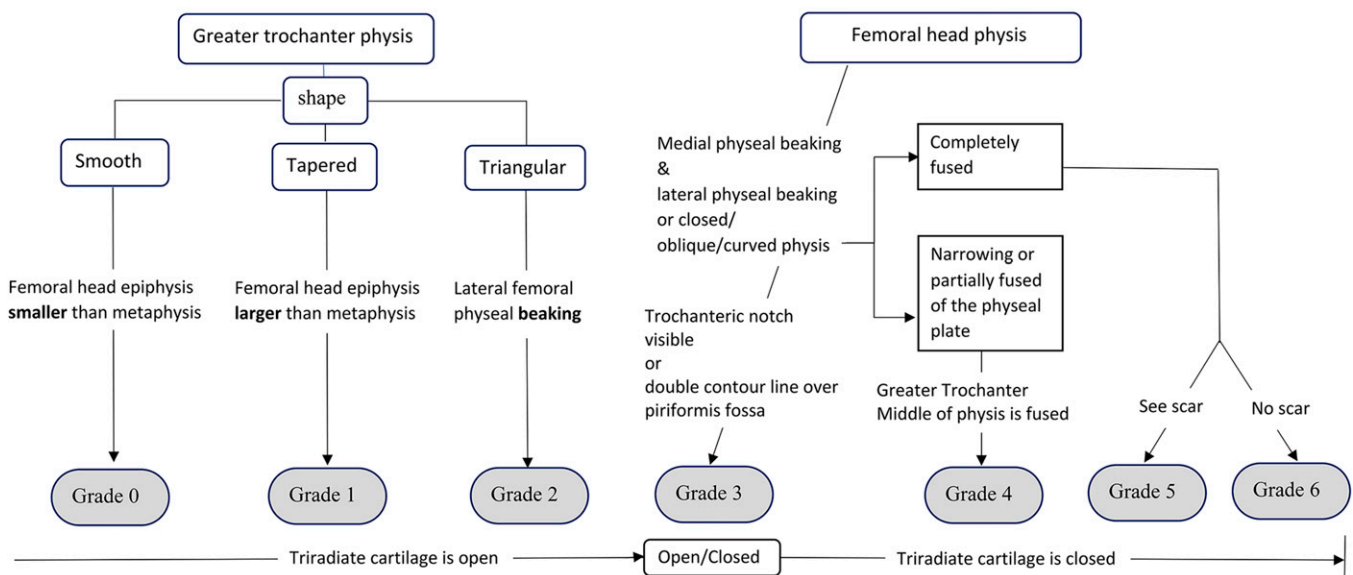


Fig. 3

Flowchart for the use of the PFMI. The classification system is used by incorporating both the femoral head and greater trochanter for final grading. Both proximal femora are checked for accuracy. If there are discrepancies between the sides, the earlier grade is used.

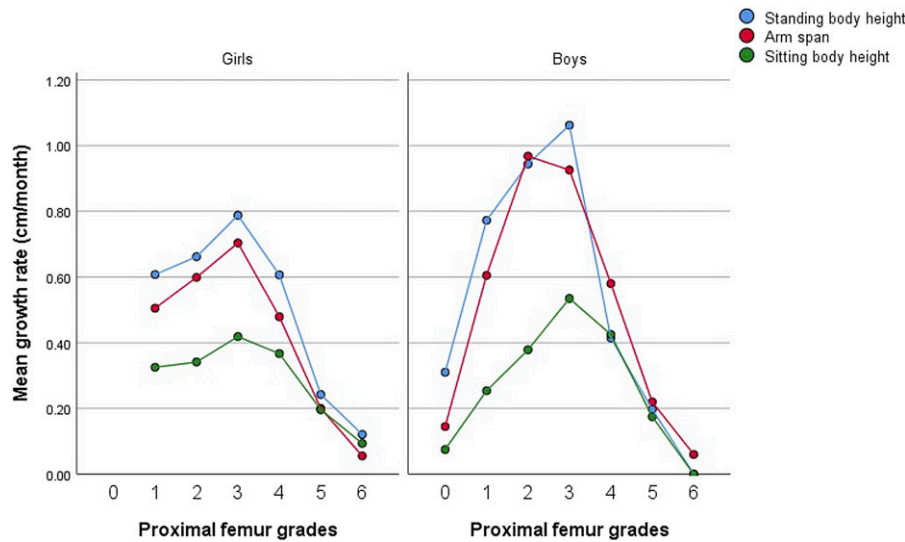


Fig. 4
Mean growth rate at each grade of the PFMI.

(see Appendix 2). Mean standing BH growth rates of 0.79 ± 0.44 cm/mo (girls) and 1.06 ± 0.67 cm/mo (boys) were observed as the peak growth rates at PFMI grade 3. Conversely, mean growth rates of 0.12 ± 0.23 cm/mo (girls) and 0 ± 0 cm/mo (boys) occurred at PFMI grade 6, indicating growth cessation. Peak growth rates (by mean values) were observed at Risser stage 0+ and 0-, SS2 and 3, R6, U5, and PHOS stage 3 for girls, and at Risser stage 0+, SS3, R6/R7, U5, and PHOS stage 3 for boys. Growth cessation occurred at Risser stage 4 (girls) and Risser

stage 5 (boys) and at SS8, R10, and U8 for both sexes. No growth occurred at PHOS stage 5 for girls but this was uncertain for boys.

Within the PFMI, there were significant differences of growth rates between PFMI grades $\chi^2[6] = 64.766$ [$p < 0.001$] for standing BH, $\chi^2[6] = 42.113$ [$p < 0.001$] for sitting BH, and $\chi^2[6] = 57.550$ [$p < 0.001$] for AS). Pairwise comparisons revealed that PFMI grade 3 had a significantly higher growth rate (based on standing BH) than that of grade 4 ($p = 0.022$), grade 5 ($p < 0.001$), and grade 6 ($p < 0.001$). In contrast, PFMI grade 2 did not have significantly different growth rates compared with grade 4 (based on standing BH, $p = 0.196$; and based on arm span, $p = 1.000$). PFMI grades 2 and 3 had no significant difference in growth rates ($p > 0.99$) either. PFMI grades 5 and 6 each had lower growth rates (standing BH and AS) than grades 1 to 4 ($p < 0.05$ for all). However, no difference was found between the growth rates (standing BH, sitting BH, and AS) at grades 5 and 6.

Strong correlations were found between PFMI gradings and Risser staging, SS, and DRU gradings (Table III), and moderate correlations were found with PHOS stages. For both sexes, cross-tabulation demonstrated that PFMI grade 3 corresponded to Risser stage 0 (-/+), SS2/SS3, R6/R7, U5, and PHOS stage 3 (see Appendix 3), whereas PFMI grade 6 corresponded to Risser stage 3/4, SS7/SS8, R9/R10, U7/U8, and PHOS stage 5 (Figs. 5-A and 5-B). PFMI grade 0 corresponded to patients as young as Risser stage 0-, R4, U1, SS1, and PHOS stage 1.

Longitudinal growth rates were evaluated for 80 girls and 24 boys, with a mean follow-up duration of 3.6 ± 0.8 years. At peak growth, the mean growth rates were 1.03 ± 0.36 cm/mo (based on standing BH) and 1.02 ± 0.33 cm/mo (based on AS) for girls, and 1.37 ± 0.72 cm/mo (based on standing BH) and 1.16 ± 0.27 cm/mo (based on AS) for boys. The most prevalent PFMI grade at peak growth was grade 3 for both sexes (Fig. 6). ROC analysis (Fig. 7) revealed the cutoff PFMI grade with

TABLE III Associations Between the Grades of the PFMI and Risser Staging, Sanders Staging, and the DRU Classification*

	Kendall Tau-b Correlation Coefficient Versus PFMI†	P Value
For girls		
Risser staging	0.743	<0.001
Sanders staging	0.722	<0.001
Radius gradings	0.792	<0.001
Ulnar gradings	0.777	<0.001
PHOS	0.613	<0.001
For boys		
Risser staging	0.774	<0.001
Sanders staging	0.736	<0.001
Radius gradings	0.820	<0.001
Ulnar gradings	0.821	<0.001
PHOS	0.675	<0.001

*PFMI = proximal femur maturity index, DRU = distal radius and ulna, and PHOS = proximal humerus ossification system. †Kendall τ_b correlation coefficient signified the strength of correlation; strong: $\tau_b \geq 0.7$, moderate: $0.4 \leq \tau_b < 0.7$, and weak: $\tau_b < 0.4$.

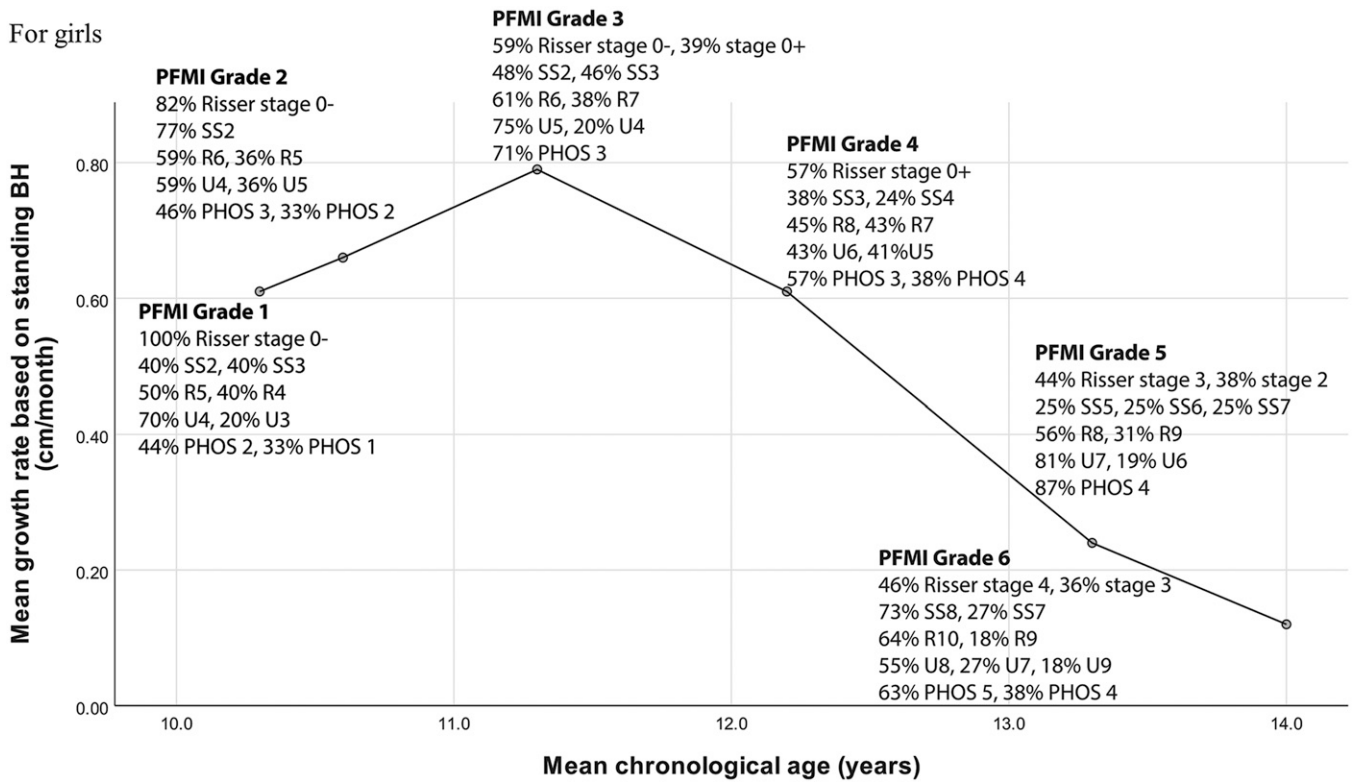


Fig. 5-A

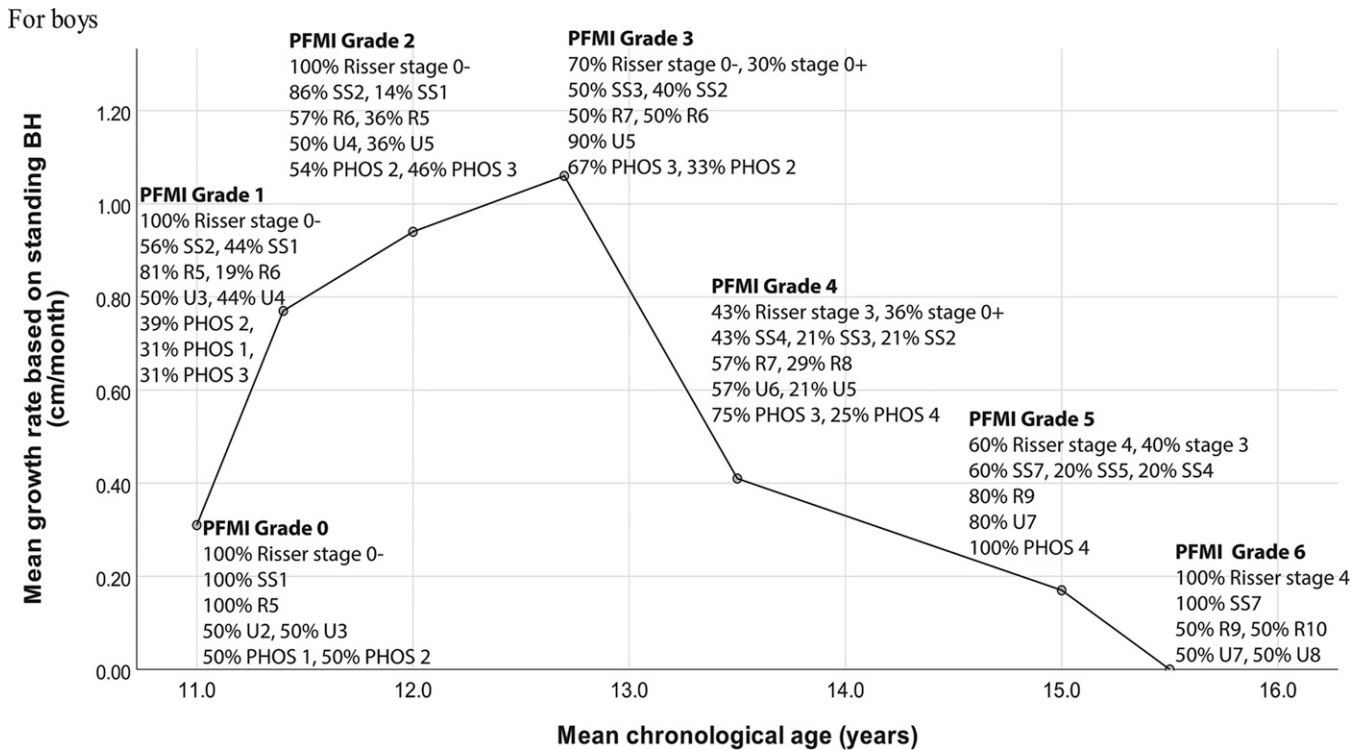


Fig. 5-B

Figs. 5-A and 5-B Cross-referencing of the PFMI gradings with Risser stages, Sanders stages (SS), radius (R) and ulnar (U) gradings, and proximal humeral ossification system (PHOS) stages; the most prevalent grade(s) (in percentages) within each skeletal maturity index are stated for girls (**Fig. 5-A**) and boys (**Fig. 5-B**). BH = body height.

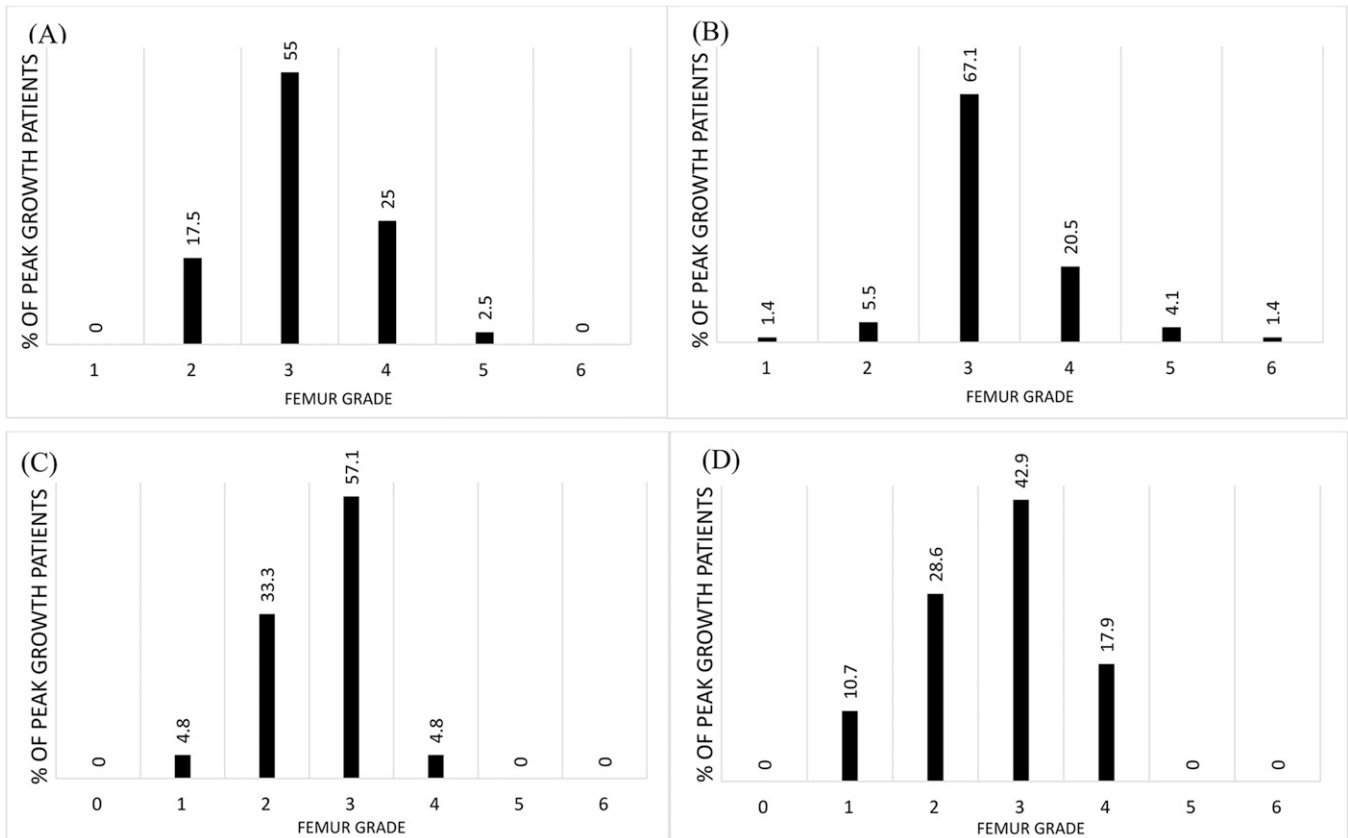


Fig. 6

Frequency of PFMI grades for peak growth based on standing BH for girls (**Fig. 6-A**), AS for girls (**Fig. 6-B**), standing BH for boys (**Fig. 6-C**), and AS for boys (**Fig. 6-D**).

highest sensitivity and specificity for predicting peak growth was grade 3.5 (Table IV).

Discussion

In this study, we established the PFMI and evaluated each stage on the basis of growth parameters as well its strong relationships with the SS, DRU classification, and Risser staging and its moderate correlation with the PHOS. The diagnostic ability and effectiveness of the PFMI grading in indicating peak growth were also evaluated on the basis of longitudinal growth data. Because of the inaccuracy of Risser staging³⁸, as well as the wish to avoid radiation exposure from hand-wrist radiographs, another growth plate with progressive epiphyseal closure in proximity to the spine is desirable.

For the whole study cohort, the PFMI was found to have a well-defined pubertal growth pattern, with acceleration, peak growth, and deceleration, from grade 0 through 6³⁹. This suggests that the proximal femoral epiphyseal maturation is representative of the adolescent growth pattern and can be used for adolescent growth assessment. Apart from the correlations found between the PFMI gradings and growth rates based on standing BH and AS, the comparison of growth rates between individual PFMI grades was important. This probing within the skeletal maturity system indicated that

PFMI grades 4, 5, and 6 each captured significantly lower growth rates than grade 3. This indicates that grade 3 is the stage when PHV takes place, and subsequent growth occurs within the growth deceleration phase (Fig. 4). Longitudinal growth data also revealed that PFMI grade 3 was the most prevalent and most predictive grading of PFMI for peak growth. For boys, however, despite the very high specificity, the cutoff PFMI grade for peak growth had relatively lower sensitivity, prompting the need for future studies with large numbers of male patients. PFMI grades 5 and 6 were found to have significantly smaller growth rates than the other grades, and thus marked the beginning of the growth plateau. The differentiation of pubertal growth into the 7 PFMI grades was shown to be capable of clearly delineating PHV from pubertal growth deceleration, and the growth plateau may begin after grade 5. However, we need to emphasize that PFMI grade 0 was rare (seen in only 2 boys) in this study cohort, which reflects the reality of unbiased subject recruitment at our scoliosis clinic. This necessitates further investigation of the use of the PFMI and its validation in scoliosis diagnosed before the age of 10 years⁴⁰, given that there is no delayed development or dysplasia of the hip, physal plate of the femoral head, or growth plate at the greater trochanter⁴¹.

Our findings also include very strong correlations of the gradings between the PFMI and the established SS, DRU

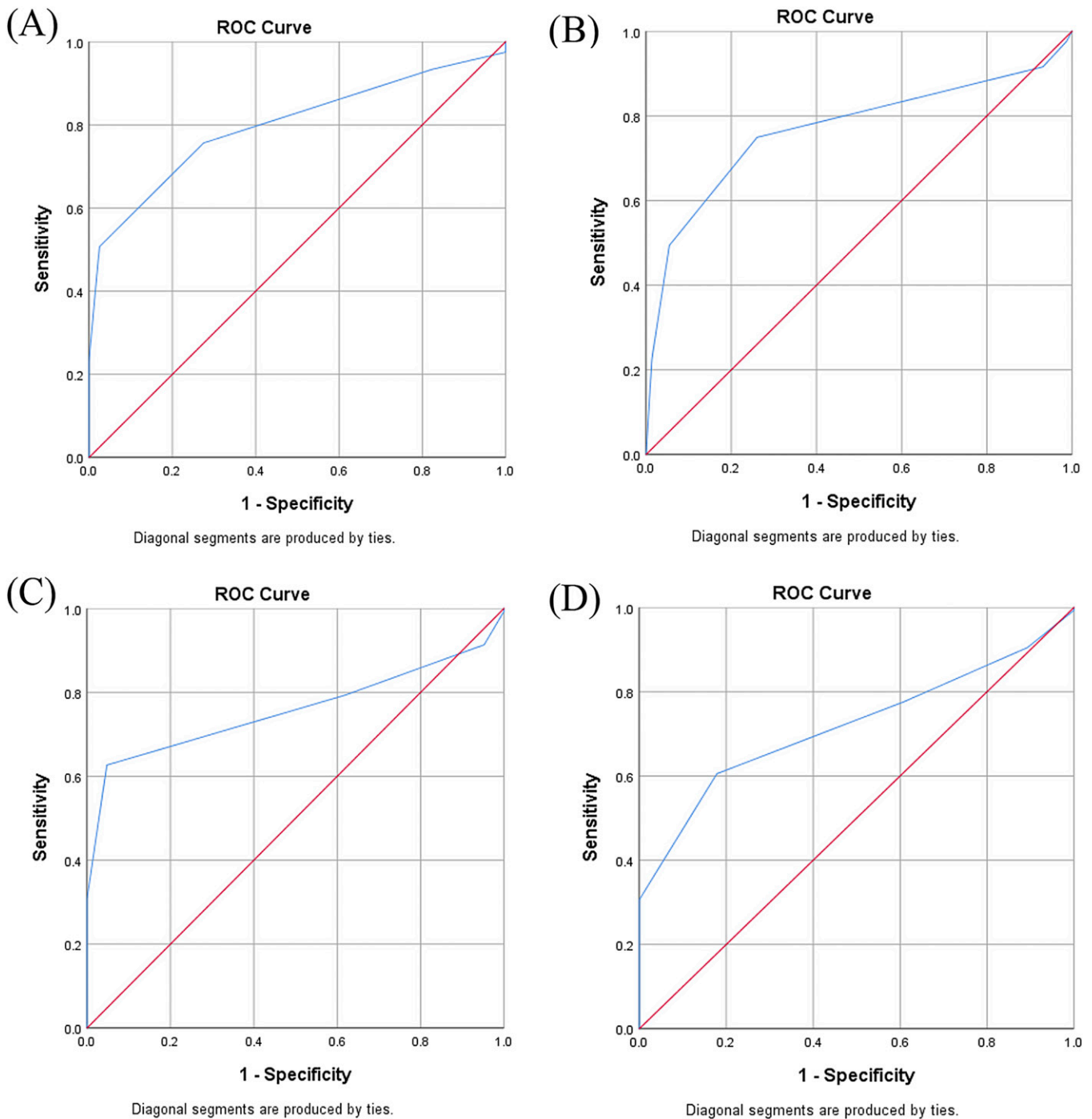


Fig. 7

The receiver operating characteristic (ROC) curve of PFMI gradings for indicating peak growth based on standing BH for girls (**Fig. 7-A**), AS for girls (**Fig. 7-B**), standing BH for boys (**Fig. 7-C**), and AS for boys (**Fig. 7-D**).

classification, and Risser staging, which are commonly used in patients with AIS. Independent analysis of these other skeletal maturity indices within this same cohort showed that PHV was located at Risser stages 0+ and 0-, SS2 and 3, R6, and U5 for girls, and at Risser stage 0+, SS3, R6/R7, and U5 for boys, being consistent with previous studies of each respective index^{15,20,42,43}.

This provides evidence that our population cohort is representative of the patients of interest, making cross-referencing with these established indices valid.

When cross-referencing among indices, PFMI grade 0 corresponded to as immature as SS1, R5, and U2 in boys and PFMI grade 1 corresponded to SS2, SS1, R4, and U1 in girls

TABLE IV Receiver Operating Characteristic (ROC) Curve Analysis for Peak Growth*

Peak Growth Based on Growth Parameters (BH and AS)	AUC†	P Value	Cutoff Grade of PFMI	Sensitivity (%)	Specificity (%)
Girls					
BH	0.805 (0.766-0.843)	<0.001	3.5	75.7	73.4
AS	0.768 (0.723-0.814)	<0.001	3.5	74.9	74.0
Boys					
BH	0.758 (0.684-0.832)	<0.001	3.5	62.7	95.2
AS	0.719 (0.638-0.800)	<0.001	3.5	60.5	82.1

*BH = standing body height, AS = arm span, AUC = area under the ROC curve, and PFMI = proximal femur maturity index. †The 95% confidence interval is given in parentheses.

(Figs. 5-A and 5-B). This demonstrates comprehensive coverage of the PFMI for peripubertal growth independent of chronological age at presentation. The uses of the PFMI in younger patients or at the prepubertal phase should be further explored.


In addition, the panel of reviewers reevaluated the newly developed index and looked for any possibility of improving its usability. A flowchart (Fig. 3) was proposed, and the ossification of the triradiate cartilage as an important anatomical feature in PFMI was emphasized (Fig. 2). Most patients (59% of girls and 70% of boys) at PFMI grade 3 still had an open triradiate cartilage, whereas all of those who reached PFMI grade 4 had a closed triradiate cartilage. Risser stage 1 only appeared at a PFMI stage of ≥ 4 , coinciding with previous findings of Risser stage 1 commonly occurring after the growth spurt²¹. The triradiate cartilage as an additional feature in this index helps improve its user-friendliness and accuracy. After introducing the flowchart and emphasizing the triradiate cartilage ossification, interrater reliability was much improved.

Limitations of this study include the lack of very immature patients in the AIS cohort, and the use of the PFMI in younger age groups should be studied. The capacity of the PFMI to estimate the risk of curve progression needs to be evaluated. Particularly, a specific study design should be tailored for studying skeletal growth assessed by the PFMI in relation to curve progression with or without intervention. The use of the PHOS and PFMI to determine growth cessation in boys requires further investigation. Also, the issue of BH loss relating to the presence of scoliosis, especially for sitting BH, should be addressed. Whether growth can be represented more accurately by using formulae for correcting BH loss^{44,45} prompts the need for in-depth probing. Future studies should also include validation of the PFMI in other ethnicities to improve its worldwide applicability⁴⁶. Moreover, despite the fact that the lower dose of radiation in biplanar stereoradiography allows scanning without the need for gonadal shields⁴⁷, there may be concerns for visualizing the proximal femur in centers with conventional imaging that requires the use of gonadal shields.

The PFMI has been established with 7 stages defined by an open physis until complete ossification of the proximal

femoral and greater trochanteric growth plates (Fig. 2). This new index can denote the acceleration and deceleration phases of the pubertal growth period and has very strong correlations with the Risser, Sanders, and DRU staging systems. The proximal femoral epiphysis is visible in routine spine radiographs, allowing skeletal maturity assessment through convenient viewing and thus avoiding additional radiation exposure. The PFMI can help to determine the timing of peak growth and growth cessation, which are important pubertal growth landmarks for the timely management of scoliosis and lower limb-length discrepancy.

Appendix

 Supporting material provided by the authors is posted with the online version of this article as a data supplement at <http://links.lww.com/JBJS/G876>. ■

Prudence Wing Hang Cheung, BDS(c)(Hons)¹

Federico Canavese, MD, PhD²

Chris Yin Wei Chan, MD, MSOrth³

Janus Siu Him Wong, MBBS, MRCSed¹

Hideki Shigematsu, MD, PhD⁴

Keith Dip Kei Luk, MBBS, MCh(Orth), FRCSEd, FRACS, FHKCOS, FHKAM¹

Jason Pui Yin Cheung, MBBS, MMedSc, MS, PDipMDPath, MD, MEd, FRCSEd, FHKAM, FHKCOS¹

¹Department of Orthopaedics and Traumatology, The University of Hong Kong, Pokfulam, Hong Kong SAR

²Pediatric Orthopedic Surgery Department, Lille University Hospital, Faculty of Medicine Henri Warembourg, University of Lille, Loos, France

³Spine Research Unit, Department of Orthopaedic Surgery (NOCERAL), Faculty of Medicine, University of Malaya, Kuala Lumpur, Malaysia

⁴Department of Orthopaedic Surgery, Nara Medical University, Nara, Japan

Email for corresponding author: cheungjp@hku.hk

References

1. Cheung JPY, Cheung PWH, Luk KD. When Should We Wean Bracing for Adolescent Idiopathic Scoliosis? *Clin Orthop Relat Res*. 2019 Sep;477(9):2145-57.
2. Mao SH, Sun X, Shi BL, Qiu Y, Qian BP, Cheng JCY. Association between braced curve behavior by pubertal growth peak and bracing effectiveness in female idiopathic scoliosis: a longitudinal cohort study. *BMC Musculoskelet Disord*. 2018 Mar 27;19(1):88.
3. Lee SC, Shim JS, Seo SW, Lim KS, Ko KR. The accuracy of current methods in determining the timing of epiphysiodesis. *Bone Joint J*. 2013 Jul;95-B(7):993-1000.
4. Birch JG, Makarov MA, Jackson TJ, Jo CH. Comparison of Anderson-Green Growth-Remaining Graphs and White-Menelaus Predictions of Growth Remaining in the Distal Femoral and Proximal Tibial Physes. *J Bone Joint Surg Am*. 2019 Jun 5;101(11):1016-22.
5. Makarov MR, Jackson TJ, Smith CM, Jo CH, Birch JG. Timing of Epiphysiodesis to Correct Leg-Length Discrepancy: A Comparison of Prediction Methods. *J Bone Joint Surg Am*. 2018 Jul 18;100(14):1217-22.
6. Baccetti T, Franchi L, De Toffol L, Ghiozzi B, Cozza P. The diagnostic performance of chronological age in the assessment of skeletal maturity. *Prog Orthod*. 2006;7(2):176-88.
7. Sanders JO, Browne RH, McConnell SJ, Margraf SA, Cooney TE, Finegold DN. Maturity assessment and curve progression in girls with idiopathic scoliosis. *J Bone Joint Surg Am*. 2007 Jan;89(1):64-73.
8. Cheung JPY, Cheung PWH, Samartzis D, Luk KD. APSS-ASJ Best Clinical Research Award: Predictability of Curve Progression in Adolescent Idiopathic Scoliosis Using the Distal Radius and Ulna Classification. *Asian Spine J*. 2018 Apr;12(2):202-13.
9. Lenz M, Oikonomidis S, Harland A, Fürnstahl P, Farshad M, Bredow J, Eysel P, Scheyerer MJ. Scoliosis and Prognosis—a systematic review regarding patient-specific and radiological predictive factors for curve progression. *Eur Spine J*. 2021 Jul;30(7):1813-22.
10. Hawary RE, Zaaroor-Regev D, Floman Y, Lonner BS, Alkhalife YI, Betz RR. Brace treatment in adolescent idiopathic scoliosis: risk factors for failure—a literature review. *Spine J*. 2019 Dec;19(12):1917-25.
11. Hacquebord JH, Leopold SS. In brief: The Risser classification: a classic tool for the clinician treating adolescent idiopathic scoliosis. *Clin Orthop Relat Res*. 2012 Aug;470(8):2335-8.
12. Dimeglio A. Growth in pediatric orthopaedics. *J Pediatr Orthop*. 2001 Jul-Aug;21(4):549-55.
13. Nault ML, Parent S, Phan P, Roy-Beaudry M, Labelle H, Rivard M. A modified Risser grading system predicts the curve acceleration phase of female adolescent idiopathic scoliosis. *J Bone Joint Surg Am*. 2010 May;92(5):1073-81.
14. Cheung PWH, Cheung JPY. Does the Use of Sanders Staging and Distal Radius and Ulna Classification Avoid Mismatches in Growth Assessment with Risser Staging Alone? *Clin Orthop Relat Res*. 2021 Nov 1;479(11):2516-30.
15. Sanders JO, Khoury JG, Kishan S, Browne RH, Mooney JF 3rd, Arnold KD, McConnell SJ, Bauman JA, Finegold DN. Predicting scoliosis progression from skeletal maturity: a simplified classification during adolescence. *J Bone Joint Surg Am*. 2008 Mar;90(3):540-53.
16. Cheung JP, Samartzis D, Cheung PW, Leung KH, Cheung KM, Luk KD. The distal radius and ulna classification in assessing skeletal maturity: a simplified scheme and reliability analysis. *J Pediatr Orthop B*. 2015 Nov;24(6):546-51.
17. Di Pauli von Treuheim T, Li DT, Mikhail C, Cataldo D, Cooperman DR, Smith BG, Lonner B. Reliable skeletal maturity assessment for an AIS patient cohort: external validation of the proximal humerus ossification system (PHOS) and relevant learning methodology. *Spine Deform*. 2020 Aug;8(4):613-20.
18. Dimeglio A, Canavese F. Progression or not progression? How to deal with adolescent idiopathic scoliosis during puberty. *J Child Orthop*. 2013 Feb;7(1):43-9.
19. Minkara A, Bainton N, Tanaka M, Kung J, DeAllie C, Khaleel A, Matsumoto H, Vitale M, Roye B. High Risk of Mismatch Between Sanders and Risser Staging in Adolescent Idiopathic Scoliosis: Are We Guiding Treatment Using the Wrong Classification? *J Pediatr Orthop*. 2020 Feb;40(2):60-4.
20. Cheung JP, Cheung PW, Samartzis D, Cheung KM, Luk KD. The use of the distal radius and ulna classification for the prediction of growth: peak growth spurt and growth cessation. *Bone Joint J*. 2016 Dec;98-B(12):1689-96.
21. Busscher I, Wapstra FH, Veldhuizen AG. Predicting growth and curve progression in the individual patient with adolescent idiopathic scoliosis: design of a prospective longitudinal cohort study. *BMC Musculoskelet Disord*. 2010 May 17;11:93.
22. Cheung JPY, Cheung PWH, Samartzis D, Luk KD. Curve Progression in Adolescent Idiopathic Scoliosis Does Not Match Skeletal Growth. *Clin Orthop Relat Res*. 2018 Feb;476(2):429-36.
23. Cheung PWH, Cheung JPY. Sanders stage 7b: Using the appearance of the ulnar physis improves decision-making for brace weaning in patients with adolescent idiopathic scoliosis. *Bone Joint J*. 2021 Jan;103-B(1):141-7.
24. Faro FD, Marks MC, Pawelek J, Newton PO. Evaluation of a functional position for lateral radiograph acquisition in adolescent idiopathic scoliosis. *Spine (Phila Pa 1976)*. 2004 Oct 15;29(20):2284-9.
25. Jean L. Influence of age and sagittal balance of the spine on the value of the pelvic incidence. *Eur Spine J*. 2014 Jul;23(7):1394-9.
26. Tardieu C, Hasegawa K, Haeusler M. How Did the Pelvis and Vertebral Column Become a Functional Unit during the Transition from Occasional to Permanent Bipedalism? *Anat Rec (Hoboken)*. 2017 May;300(5):912-31.
27. Amzallag-Bellenger E, Uyttenhove F, Nectoux E, Moraux A, Bigot J, Herbaux B, Boutry N. Idiopathic scoliosis in children and adolescents: assessment with a bi-planar X-ray device. *Insights Imaging*. 2014 Oct;5(5):571-83.
28. Stasikelis PJ, Sullivan CM, Phillips WA, Polard JA. Slipped capital femoral epiphysis. Prediction of contralateral involvement. *J Bone Joint Surg Am*. 1996 Aug;78(8):1149-55.
29. Zide JR, Popejoy D, Birch JG. Revised modified Oxford bone score: a simpler system for prediction of contralateral involvement in slipped capital femoral epiphysis. *J Pediatr Orthop*. 2011 Mar;31(2):159-64.
30. Risser JC. The iliac apophysis; an invaluable sign in the management of scoliosis. *Clin Orthop*. 1958;11(11):111-9.
31. Nault ML, Parent S, Phan P, Roy-Beaudry M, Labelle H, Rivard M. A modified Risser grading system predicts the curve acceleration phase of female adolescent idiopathic scoliosis. *J Bone Joint Surg Am*. 2010 May;92(5):1073-81.
32. Mandrekar JN. Measures of interrater agreement. *J Thorac Oncol*. 2011 Jan;6(1):6-7.
33. Ranganathan P, Pramesh CS, Aggarwal R. Common pitfalls in statistical analysis: Measures of agreement. *Perspect Clin Res*. 2017 Oct-Dec;8(4):187-91.
34. Cicchetti DV, Allison T. A New Procedure for Assessing Reliability of Scoring EEG Sleep Recordings. *American Journal of EEG Technology*. 1971;11(3):101-10.
35. Vanbelle S. A New Interpretation of the Weighted Kappa Coefficients. *Psychometrika*. 2016 Jun;81(2):399-410.
36. Fleiss JL, Paik MC, Levin B. *Statistical Methods for Rates and Proportions*. 3rd ed. John Wiley & Sons; 2003. p 609.
37. Akoglu H. User's guide to correlation coefficients. *Turk J Emerg Med*. 2018 Aug 7;18(3):91-3.
38. Yang JH, Bhandarkar AW, Suh SW, Hong JY, Hwang JH, Ham CH. Evaluation of accuracy of plain radiography in determining the Risser stage and identification of common sources of errors. *J Orthop Surg Res*. 2014 Nov 19;9:101.
39. Soliman A, De Sanctis V, Elalaily R, Bedair S. Advances in pubertal growth and factors influencing it: Can we increase pubertal growth? *Indian J Endocrinol Metab*. 2014 Nov;18(Suppl 1):S53-62.
40. Helenius IJ. Treatment strategies for early-onset scoliosis. *EFORT Open Rev*. 2018 May 21;3(5):287-93.
41. Weinstein SL, Dolan LA. Proximal femoral growth disturbance in developmental dysplasia of the hip: what do we know? *J Child Orthop*. 2018 Aug 1;12(4):331-41.
42. Sanders JO, Qiu X, Lu X, Duren DL, Liu RW, Dang D, Menendez ME, Hans SD, Weber DR, Cooperman DR. The Uniform Pattern of Growth and Skeletal Maturation during the Human Adolescent Growth Spurt. *Sci Rep*. 2017 Dec 1;7(1):16705.
43. Little DG, Song KM, Katz D, Herring JA. Relationship of peak height velocity to other maturity indicators in idiopathic scoliosis in girls. *J Bone Joint Surg Am*. 2000 May;82(5):685-93.
44. Tyrakowski M, Kotwicki T, Czubak J, Siemionow K. Calculation of corrected body height in idiopathic scoliosis: comparison of four methods. *Eur Spine J*. 2014 Jun;23(6):1244-50.
45. Gardner A, Price A, Berryman F, Pynsent P. The use of growth standards and corrective formulae to calculate the height loss caused by idiopathic scoliosis. *Scoliosis Spinal Disord*. 2016 Feb 26;11:6.
46. Zhang A, Sayre JW, Vachon L, Liu BJ, Huang HK. Racial differences in growth patterns of children assessed on the basis of bone age. *Radiology*. 2009 Jan;250(1):228-35.
47. Hui SCN, Pialasse JP, Wong JYH, Lam TP, Ng BKW, Cheng JCY, Chu WC. Radiation dose of digital radiography (DR) versus micro-dose x-ray (EOS) on patients with adolescent idiopathic scoliosis: 2016 SOSORT-IRSSD "John Sevastic Award" Winner in Imaging Research. *Scoliosis Spinal Disord*. 2016 Dec 29;11:46.